Typhoon-induced precipitation impact on nutrient and suspended matter dynamics of a tropical estuary affected by human activities in Hainan, China

Lucia S. Herbeck [a,*], Daniela Unger [a], Uwe Krumme [a], Su Mei Liu [b], Tim C. Jennerjahn [a]

[a] Leibniz Center for Tropical Marine Ecology (ZMT), Fahrenheitstraße 6, 28359 Bremen, Germany
[b] Key Laboratory of Marine Chemistry Theory and Technology, Ministry of Education, College of Chemistry and Chemical Engineering, Ocean University of China, Qingdao 266100, China

ARTICLE INFO

ABSTRACT

Typhoons regularly hit the coasts along the northern South China Sea during summer monsoon. However, little is known on the effects of typhoon-related heavy precipitation on estuarine dynamics and coastal ecosystems. We analyzed physico-chemical characteristics, and concentrations and composition of dissolved and suspended matter in the Wenchang/Wenjiao Estuary (WWE) on the tropical island of Hainan, China, prior to and after typhoon Kammuri in August 2008. Before the typhoon, the estuary displayed vertical and horizontal gradients. High nutrient inputs from agriculture and widespread aquaculture were to a large extent converted into biomass inside the estuarine lagoon resulting in low export of nutrients to coastal waters and a mainly autochthonous origin of total suspended matter (TSM). Heavy typhoon-associated precipitation increased river runoff, which moved the location of the estuarine salinity gradient seaward. It resulted in an export of dissolved and particulate matter to coastal waters one day after the typhoon. Dissolved nutrients increased by up to an order of magnitude and TSM increased approximately twofold compared to pre-typhoon values. Lower $\delta^{13}C_{org}$ and $\delta^{15}N$ and elevated C/N ratios of TSM together with lower chlorophyll a (chl a) concentrations indicated an increased contribution of terrestrial material originating from typhoon-induced soil erosion. Local uptake of excess nutrients inside the lagoon was inhibited because of reduced water transparency and the lack of phytoplankton, which had been washed out by the initial freshwater pulse. Two weeks after the typhoon, TSM concentration and composition had almost returned to pre-typhoon conditions. However, physico-chemical properties and nutrients were still different from pre-typhoon conditions indicating that the estuarine system had not fully recovered. Unusually high chl a concentrations in the coastal zone indicated a phytoplankton bloom resulting from the typhoon-induced nutrient export. The typhoon-induced flushing of the WWE resulted in hyposalinity, reduced water transparency, siltation, as well as temporary eutrophication of coastal waters. These are physiological stressors, which are known to impair the performance of adjacent seagrass meadows and coral reefs. The predicted increase in typhoon frequency and intensity will lead to a frequently recurring exposure of coastal ecosystems to these threats, particularly in the South China Sea region where aquaculture is widespread and tropical cyclone frequency is at a maximum.

© 2011 Elsevier Ltd. All rights reserved.

1. Introduction

Tropical storms, also known as typhoons, hurricanes and cyclones, are among the most extreme episodic weather events affecting wetlands and adjacent marine and coastal areas in low latitudes. Usually, tropical storms are accompanied by heavy precipitation, which can occur even several hundreds of kilometers away from the storm's center. Their strength and frequency are predicted to increase in the context of global climate change (Goldenberg et al., 2001; Emanuel, 2005; Webster et al., 2005; Wu et al., 2005; Knutson et al., 2010).

Effects of tropical storms on estuaries and nearshore coastal systems remain poorly studied, partly because of the unpredictability of storm formation and tracks, which make it difficult to arrange for appropriate pre- and post-storm sampling. Additionally, harsh weather conditions often make timely sampling difficult,

especially as some effects may already dissipate after a few days (e.g. Valiela et al., 1998). Existing studies have mostly been conducted in large temperate and subtropical estuaries and nearshore coastal areas in highly developed regions (mainly on hurricane events in the USA, e.g. Pamlico Sound, Biscayne Bay), where comprehensive background data exist. These studies reported on changes in salinity, nutrient supply and primary productivity, as well as on modifications of TSM load and composition driven by storm precipitation (Valiela et al., 1998; Paerl et al., 2001, 2006a; Peierls et al., 2003; Burkholder et al., 2004; Wetz and Paerl, 2008; Piazza and La Peyre, 2009; Zhang et al., 2009). Storm-related perturbations have been found to intensify with the amount of rainfall, as well as with land use intensity and population density of the drainage basin (Valiela et al., 1998; Mallin et al., 1999; Paerl et al., 2001, 2006a, 2006b; Mallin and Corbett, 2006). The impact and persistence of such episodic events in estuarine and coastal systems, however, has to be evaluated locally, as they depend on drainage basin size, land use, estuary size and shape, water residence time, tidal effects etc (e.g. Paerl et al., 2006a; Wolanski, 2007).

With an average of 26.9 ± 4.3 tropical storms per year, the tropical/subtropical Western Pacific is the most active typhoon basin of the world (Fink and Speth, 1998; Wang et al., 2010). Studies from this region mostly relate to typhoon effects in offshore waters, where phytoplankton blooms were observed as a consequence of wind-driven upwelling and mixing, as well as assumed nutrient input from rivers (Shiah et al., 2000; Lin et al., 2003; Zheng and Tang, 2007; Zhao et al., 2009; Sun et al., 2010). Knowledge from the pacific region on the effects of typhoons on river, estuarine and nearshore coastal dynamics is mainly limited to Taiwan (e.g. Kao and Liu, 1996; Chen et al., 2001; Milliman and Kao, 2005; Milliman et al., 2007; Goldsmith et al., 2008; Hilton et al., 2008), while almost nothing is known on typhoon effects on coastal tropical habitats, such as mangroves, seagrass meadows and coral reefs (Wolanski et al., 2003; Victor et al., 2006). These tropical regions often experience particularly intense anthropogenic stress from high population density and ongoing land use change, which is projected to further increase in the future (Seitzinger et al., 2002). As in many other parts of tropical SE Asia, mangroves in China have been replaced to a large extent by paddy fields and aquaculture ponds (Li and Lee, 1997). These and other activities contribute to eutrophication, one of the most problematic anthropogenic impacts on estuarine and coastal waters worldwide (Turner and Rabalais, 1994; Vitousek et al., 1997; Justic et al., 2002; Diaz and Rosenberg, 2008). Resulting adverse effects, such as reduced water transparency, formation of hypoxia, altered nutrient ratios and cycling, as well as toxic algal blooms, contribute to the degradation of coastal habitats (Vitousek et al., 1997; Rabalais and Gilbert, 2009). Increased sediment input caused by soil erosion from deforested watersheds threatens estuarine and coastal water quality and habitats. This is further accelerated by the loss of mangrove forests (e.g. Wattayakorn et al., 1990; Alongi, 2002; Victor et al., 2004, 2006; Thampanya et al., 2006; Wolanski, 2007).

Here, we report on the effects of a typhoon on the biogeochemistry of the tropical Wenchang/Wenjiao Estuary (WWE) and its adjacent coastal zone at the east coast of Hainan, northern South China Sea. The region is the major landfall corridor of typhoons in
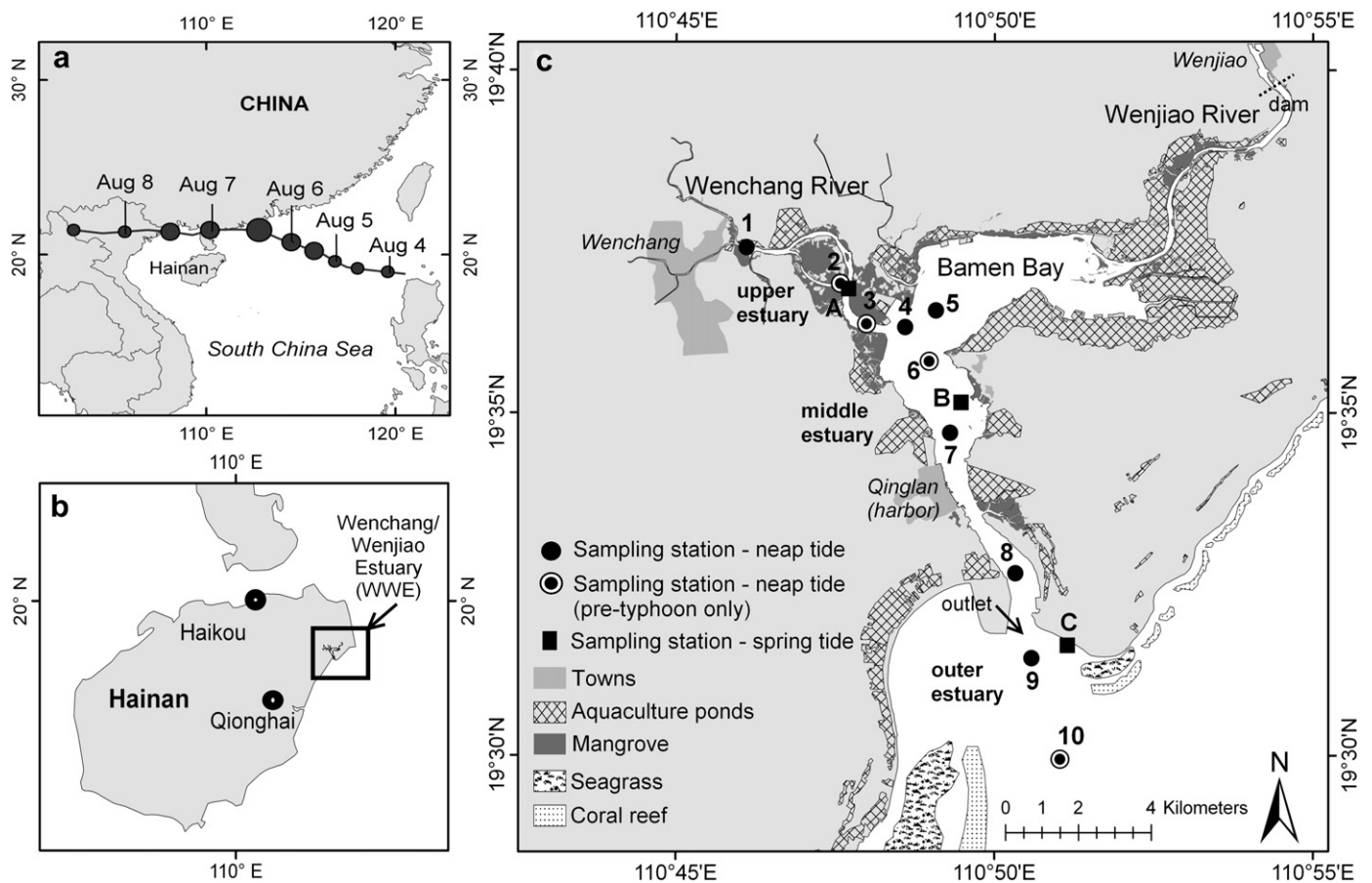

Fig. 1. Locations of (a) Hainan Island and passage track of typhoon Kammuri (position date calculated as UTC+8h; Kitamoto, 2011), (b) the Wenchang/Wenjiao Estuary (WWE), east coast of Hainan, and weather stations (Haikou and Qionghai) and (c) the Wenchang/Wenjiao Estuary (WWE) and adjacent nearshore coastal zone including sampling stations at neap tide (1–10) and spring tide (time series tidal cycle, A–C).

Hainan (Zeng and Zeng, 1989) and has experienced intense land use changes in its watershed, most notably the conversion of mangroves into aquaculture ponds. We compare sources and processes affecting nutrients and suspended matter along the estuary during two weeks before and two weeks after typhoon-induced heavy precipitation and evaluate the potential impact on nearby seagrass meadows and fringing coral reefs.

2. Materials and methods

2.1. Study area

Hainan is the largest Chinese island in the South China Sea, located in the marginal tropics (Fig. 1a). The Wenchang/Wenjiao Estuary (WWE) is situated at Hainan's east coast (19°36′ N, 110°49′ E) and comprises an area of approximately 40 km² (Fig. 1b and c). The lowland rivers Wenchang and Wenjiao enter the shallow (mean depth: 3 m), kidney-shaped lagoon Bamen Bay, which is connected to the sea via a narrow natural channel (maximum depth: 10 m; Fig. 1c). The estuary is subject to mixed semidiurnal microtides. The tidal range at spring and neap tides is around 1.5 m and 0.5, respectively (Fig. 2). Hence, we can expect stronger tidal mixing during spring tides. Neap tides are semidiurnal, whereas spring tides are mixed semidiurnal (Fig. 2). In the lagoon the currents are clearly bi-directional, upstream at flood and downstream at ebb tides. At spring tides, flood current speeds reached a maximum of 0.3 m s^{-1}, while ebb tide current speeds could exceed 0.6 m s^{-1}, so that the system is ebb-dominated during this period (Ye, 1988; Krumme et al., under review). There are no reliable data on water discharge of the estuary available. Krumme et al. (under review) estimated a water residence time of 5.6 days using the empirical formula of Uncles et al. (2002).

The WWE can be divided into three zones: the upper estuary, including the lower reaches of the rivers Wenchang and Wenjiao, the middle estuary, covering the lagoon and the channel, and the outer estuary, which is located in the nearshore coastal zone (Fig. 1c). The watersheds of the rivers Wenchang and Wenjiao are characterized by mixed agriculture dominated by rice, coconut palm and fruit cultures (mainly C3 plants). The Wenchang River passes the county capital Wenchang (55.800 inhabitants in 2009; Fig. 1) and enters the lagoon in the north-west. Since the Wenjiao River at the north-east of the lagoon is dammed, the Wenchang brings the major freshwater input, as well as untreated urban effluents and sediments into the system. 73% of the fringing riverine mangrove has been lost since the 1960s (Krumme et al., under review) and has been replaced by aquaculture ponds with semi-intensive and intensive shrimp and fish culture, which now cover approximately 15 km² (~35%) of the lagoon (Fig. 1c). Despite some mangrove remnants that fringe the pond complexes on their seaward edge, the former mangrove area has lost its ecological function as filter and sediment trap. Instead, the area has become a major source of untreated effluents, released into the estuary from aquaculture ponds. On top of that, feces and excess feed are discharged from hundreds of floating net cages containing live fishes and invertebrates that are mainly lined up opposite of Qinglan harbor. In the outer estuarine zone, fringing coral reefs occur in a few hundred meters offshore and seagrass meadows are found in their back-reef areas (Fig. 1c).

The region is characterized by a tropical monsoon climate with a dry season from November to April and a wet season from May to October (Fig. 2a). The annual average air temperature is 22–26 °C, the coldest monthly average air temperature is 15.3 °C (Wang, 2002). Between 1959 and 2000, Hainan Island was impacted by an annual mean of 7.9 typhoons and directly hit by 2.6 typhoons (Liu, 1984 cited in Huang, 2003). The north-eastern Wenchang-

Haikou region has the highest frequency of typhoon landfall incidents on the island (Zeng and Zeng, 1989), where typhoon-induced rainfall accounts for 35–60% (>700 mm) of the total annual precipitation of 1500–2000 mm (Huang, 2003; Wang et al., 2008). Typhoon activity on the island lasts from June to November with the peak frequency between July and September, when extreme rainfall alternates with dry periods of several weeks (Fig. 2a; Zeng and Zeng, 1989; Wang et al., 2010).

2.2. Typhoon Kammuri

Kammuri developed as a tropical depression in the northern South China Sea north of the Philippine island of Luzon on August 4, 2008 (Fig. 1a). During its passage toward mainland China, Kammuri developed into a severe tropical storm as categorized by the Hong Kong Observatory (HKO) and the Japan Meteorological Agency (JMA) in the late evening of August 5. Kammuri made landfall along the South coast of China in the Western Guangdong Province (close to Hong Kong) at about 12 pm UTC on August 6. It passed the study area in a distance of approximately 200 km in the night to August 7 before it moved into the Gulf of Tonkin. It made landfall for a second time in the Guangxi Province, China, before it dissipated on August 8. The maximum radius of gale wind was 440 km with maximum sustained wind speeds of 95 km h^{-1} (Kitamoto, 2011). Although, according to the Saffir-Simpson Hurricane Scale and the storm scale of Japan Meterological Agency, Kammuri was classified as a severe tropical storm, the denomination 'typhoon Kammuri' was commonly used. Therefore, we will also use the term 'typhoon'.

No precipitation data are available for the Wenchang region, but our observations showed that Kammuri caused a first peak of heavy rain on August 6, followed by a second peak on August 9. Precipitation records from weather stations in Haikou and Qionghai (Fig. 1b) reveal that heavy precipitation of 40–145 mm per day were a widespread phenomenon during the passage of Kammuri (Fig. 2b). As typhoon Kammuri passed the study area in quite a distance, heavy precipitation was expected to be the major pressure on the system, while wind-driven effects were of minor importance (own observations).

2.3. Sampling design

Sampling in the WWE took place in July/August 2008 with two sampling campaigns before and two after the passage of typhoon Kammuri (Fig. 2b). Sampling focused on the western part of the lagoon and the lower reaches of the Wenchang River (Fig. 1c). The Wenjiao River is dammed, which results in negligible river discharge. Sampling at neap tides (13 days before and 1 day after the typhoon) included collection of surface water, suspended matter and physico-chemical measurements by boat and was carried out along the WWE at 10 stations before and 6 stations after the typhoon (Fig. 1c). Additionally, bottom water was collected at some stations in the middle and outer estuary, where water depth was ≥3 m. Both neap tide cruises were conducted at similar tide levels between low and high tide (55–90 cm). Sampling at spring tides (4–9 days before and 7–12 days after the typhoon) was conducted at three fixed stations along the WWE (Figs. 1 and 2): stations A (upper estuary), B (middle estuary) and C (outer estuary). Each station was sampled over a 24 h period. Physico-chemical parameters were measured in situ and samples for the analysis of dissolved and suspended matter of surface water were taken every 3 h from an anchored boat, yielding $n = 8$ per parameter per tidal cycle. In addition to spring and neap tide sampling campaigns, water, suspended matter, sediment, soil and plant samples were collected before the typhoon at different locations along the estuary and the watershed.
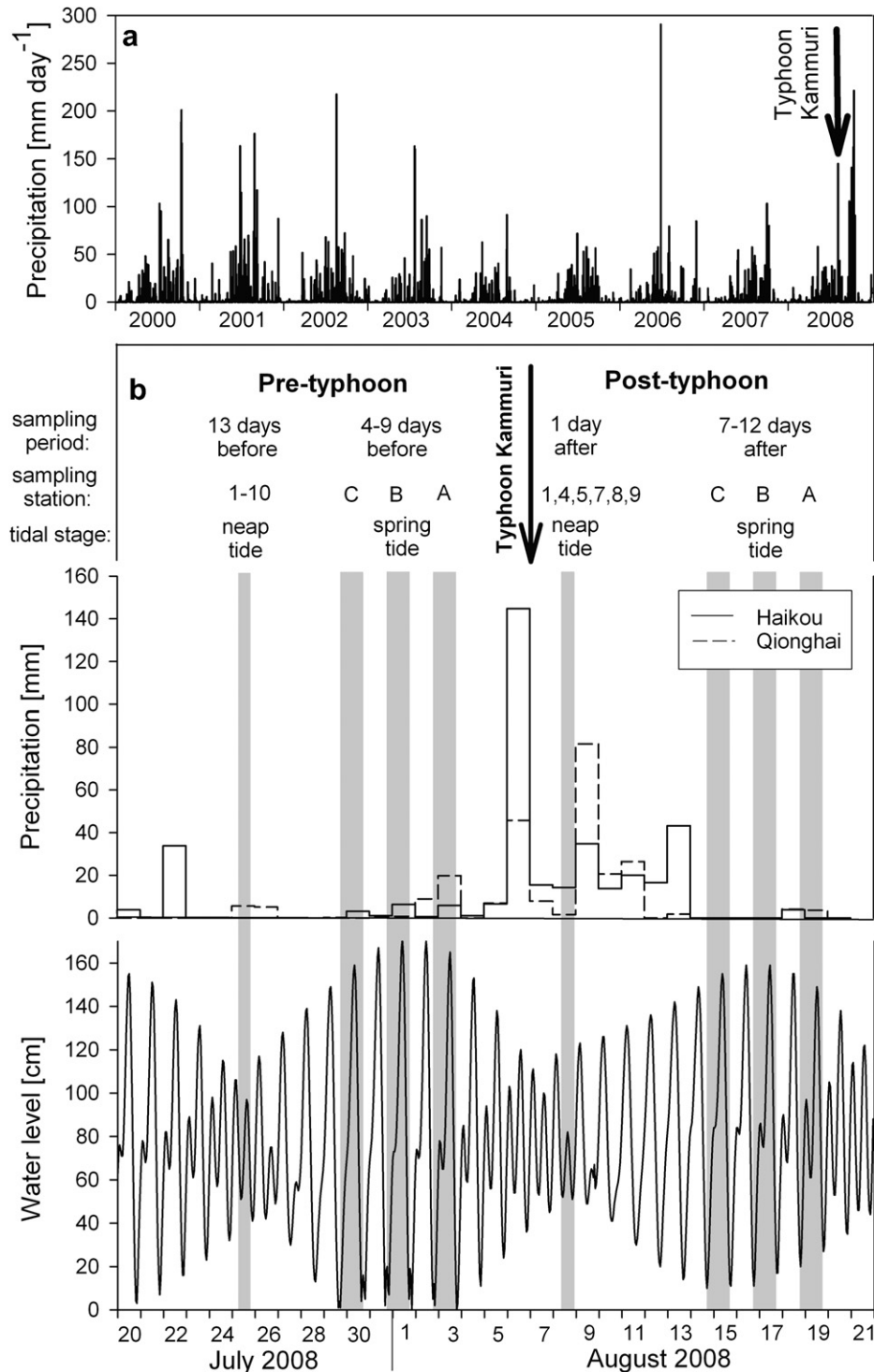
Fig. 2. (a) Daily precipitation at the weather station Haikou from 2000 to 2008; (b) zoom-in of the sampling time in July/August 2008: daily precipitation at the weather stations in Haikou and Qionghai (upper panel) and time series of tidal changes in water level (lower panel) in the WWE during the pre- and post-typhoon Kammuri phase (for location of station names see Fig. 1c). Precipitation data from Climate Center (2011); (locations of weather stations see Fig. 1b); water level data from tidal calendar predictions for Qinglan (real water levels were approximately 1–2 m higher during the typhoon).

2.4. Data collection and sample preparation

Salinity (±0.1), water temperature (±0.1 °C) and pH (±0.1) were measured in situ with a WTW MultiLine F/Set3 multi-parameter probe and dissolved oxygen (DO; ±0.02 mg l^{-1}) was measured with a LDO™ HQ40d portable dissolved oxygen meter. Vertical Secchi depth readings were taken during daylight hours

(06:00–18:00). Water samples were collected with a bucket and a Niskin bottle for surface and bottom water, respectively. Water samples for nutrient analyses were filtered immediately after sampling through single use Sartorius Minisart® membrane filters (0.45 μm pore size) into PE bottles, which were rinsed three times with the filtered sampling water beforehand. Samples were preserved with a mercury chloride solution (50 μl of a 20 g l^{-1}
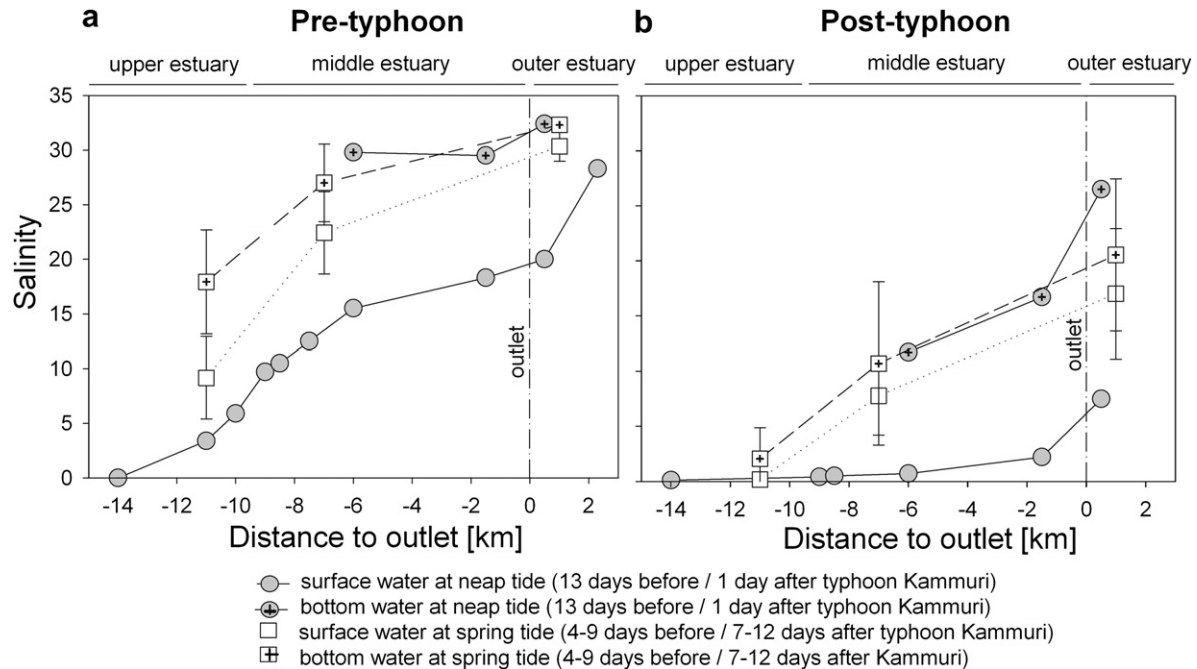
Fig. 3. Surface and bottom water salinities along the WWE under (a) neap and spring tide pre-typhoon and (b) neap and spring tide post-typhoon conditions. Spring tide samples with mean and standard deviation ($n = 8$).

HgCl$_2$-solution added to 100 ml sample) and stored cool and dark until analysis. Water samples for the analysis of total suspended matter (TSM) were stored in PE tanks until filtration in the laboratory the same day. Samples were filtered under constant pressure onto pre-combusted (5 h, 450 °C) and pre-weighed Whatman GF/F filters and dried at 40 °C. For chlorophyll a (chl a) analysis, water was filtered onto GF/F filters, which were stored frozen until analysis within the following days. Samples of surface sediments and soils were collected directly with a spoon, where possible, or with a grab sampler and stored cool in plastic bags or glass vials. Each plant sample consisted of 2−10 fresh leaves of a plant, which were rinsed and stored in plastic bags. All sediment, soil and plant samples were dried in a drying oven at 40 °C within the same day after collection.

2.5. Analyses

Dissolved nutrients were analyzed using a continuous flow analyzing system (Skalar SAN^{++}System). Nitrate + Nitrite (NO$_x^-$),

nitrite (NO$_2^-$), phosphate (PO$_4^{3-}$) and silicate (Si(OH)$_4$) were detected spectrophotometrically and ammonium (NH$_4^+$) fluorometrically as colored/fluorescence dye (Grasshoff et al., 1999). Nitrate (NO$_3^-$) is NO$_x^-$ − NO$_2^-$. Dissolved inorganic nitrogen (DIN) is the sum of NO$_3^-$, NO$_2^-$ and NH$_4^+$. Daily equidistant 10 point calibrations for the necessary concentration ranges were established. Detection limits of the procedure were 0.03 μM, 0.01 μM, 0.02 μM, 0.02 μM, and 0.06 μM for NO$_x^-$, NO$_2^-$, NH$_4^+$, PO$_4^{3-}$ and Si(OH)$_4$, respectively; determination limits were 0.08 μM, 0.04 μM, 0.06 μM, 0.07 μM and 0.19 μM, respectively, according to DIN 32645 (German Institute of Standardization). The coefficient of variation of the procedure was <3.4%. For chlorophyll a (chl a) determination, pigments were extracted from the filters in 10 ml 90% acetone at 4 °C in the dark for approximately 24 h and vials were shaken once in a while. Extracts were centrifuged at 60 rpm for 3 min. The supernatant was measured with a Lovibond PC Spectro 1.0 photometer (Tintometer GmbH) and chl a concentrations were calculated according to the method of Lorenzen (1967). Concentrations of total suspended matter (TSM) were determined by

Table 1
Physico-chemical characteristics of the surface water in the upper, middle and outer regions of the WWE under pre- and post-typhoon conditions during neap and spring tide. Spring tide samples with mean and standard deviation ($n = 8$).

Pre/post-typhoon	upper estuary		middle estuary		outer estuary	
	pre	post	pre	post	pre	post
Neap tide						
Station	1	1	7	7	9	9
Salinity	0.0	0.1	15.5	0.7	20.0	7.5
Temperature [°C]	33.7	28.1	31.7	27.8	30.5	27.4
pH	7.3	7.8	8.5	8.3	8.4	8.0
DO [mg L^{-1}]	6.7	5.7	8.5	6.2	6.9	6.5
Secchi depth [m]	0.7	0.3	1.0	0.3	1.8	0.6
Spring tide						
Station	A	A	B	B	C	C
Salinity	9.2 (±3.7)*	0.2 (±0.4)	22.4 (±3.8)*	7.8 (±3.6)	30.3 (±1.4)*	17.0 (±6.0)
Temperature [°C]	31.0 (±0.9)	30.7 (±0.8)	31.4 (±0.8)	31.1 (±0.5)	30.9 (±1.2)	30.0 (±1.1)
pH	7.3 (±0.4)*	5.9 (±0.7)	8.1 (±0.1)*	8.4 (±0.1)	8.1 (±0.1)	8.2 (±0.1)
DO [mg L^{-1}]	4.5 (±2.0)	5.5 (±0.4)	7.5 (±0.8)*	9.2 (±1.5)	8.4 (±1.3)	9.0 (±1.0)
Secchi depth [m]	1.0 (±0.2)*	0.7 (±0.2)	1.1 (±0.2)	0.8 (±0.3)	>1.2 (±0.5)	1.1 (±0.4)

* Values are significantly different (t-test for independent samples by group; $p < 0.05$).

weighing the dried filter, subtracting the original weight of the empty filter and dividing it by the respective volume of water filtered. Values given are the average of 3–5 filters. TSM on GF/F filters was analyzed for total carbon (C_{tot}) and total nitrogen (TN) by high-temperature combustion in a Carlo Erba NA 2100 elemental analyzer (Verardo et al., 1990). Organic carbon (C_{org}) was determined the same way after removal of carbonate by acidification with 1 N HCl and subsequent drying at 40 °C. Measurements had a precision of 0.06% for C_{org} and 0.02% for TN, based on repeated measurements of a standard (LECO 1012). The nitrogen isotope composition ($\delta^{15}N$) was determined with a Thermo Finnigan Delta Plus gas isotope ratio mass spectrometer after high-temperature combustion in a Flash 1112 EA elemental analyzer. The carbon isotope composition ($\delta^{13}C_{org}$) was determined similarly after removal of carbonates by adding 1 N HCl and subsequent drying at 40 °C. $\delta^{13}C_{org}$ and $\delta^{15}N$ are given as ‰-deviation from the carbon isotope composition of the PDB standard and the nitrogen isotope composition of atmospheric air, respectively. The precisions of the method, measured by an internal standard, were 0.20‰ ($\delta^{15}N$) and 0.14‰ ($\delta^{13}C_{org}$). Dried sediment, soil and plant material was analyzed for C_{org}, TN, $\delta^{13}C_{org}$ and $\delta^{15}N$ contents following the same procedure as described for filters after homogenizing and grinding to a fine powder in a planet mill. For each spring tide station, means and standard deviations of the 8 measurements were calculated and water parameters were tested for differences between pre- and post-typhoon conditions using the *t*-test for independent samples by groups ($p < 0.05$; STATISTICA 9).

3. Results

3.1. Physico-chemical characteristics

Before the typhoon, the salinity gradient was mainly located within the middle estuary with brackish water reaching up to station 2/A in the Wenchang River (upper estuary; Fig. 3a; Table 1). Only at station 1 during neap tide, surface water salinity was 0. Bottom water salinities were always higher than surface salinities, indicating water column stratification along the estuary. During spring tide, surface water salinities were higher than during neap tide and differences between surface and bottom water salinities were smaller (Fig. 3a). Surface water temperature, pH, DO and Secchi depth showed a clear trend along the estuarine gradient and hardly varied for neap and spring tide (Table 1). High standard deviations of most parameters at stations A–C reflected large tide-induced changes during 24 h sampling at spring tide, especially in the upper estuary. Here, DO values, which were relatively high in the middle and outer estuary (>6.5), decreased to up to 2.7 mg L^{-1} during the night.

One day after landfall of typhoon Kammuri (August 8, see Fig. 2b) during neap tide, surface water salinity had dropped to values <3 throughout the upper and middle estuary, while in the outer estuary, surface salinity was 7.5 compared to 20 before the typhoon (Fig. 3b). Estuarine stratification still persisted but bottom water salinities were lower than under pre-typhoon conditions (Fig. 3) indicating that tidal mixing was minimal and the entire estuary was dominated by freshwater. Surface water temperature, pH, DO and Secchi depth were considerably lower at all stations immediately after the typhoon and the variability in water parameters from the river to the coast was less pronounced (Table 1).

Spring tide measurements at stations A–C showed that one to two weeks after the typhoon (August 14–19, see Fig. 2b), salinity, water temperature, pH, DO and Secchi depth had started to rise again compared to immediately after the typhoon at most of the stations (Fig. 3b; Table 1). However, salinity was still significantly

lower compared to pre-typhoon spring tide conditions and also average temperature and Secchi depths were below pre-typhoon values. Average pH and DO in the middle and outer estuary were elevated compared to pre-typhoon values during spring tide. A very low variability of salinity at station A as compared to before the typhoon indicates that the upper estuary was still dominated by freshwater during most of the spring tidal cycle, while large standard deviations at stations B and C reflect tidal mixing in the lower parts of the estuary (Fig. 3; Table 1).
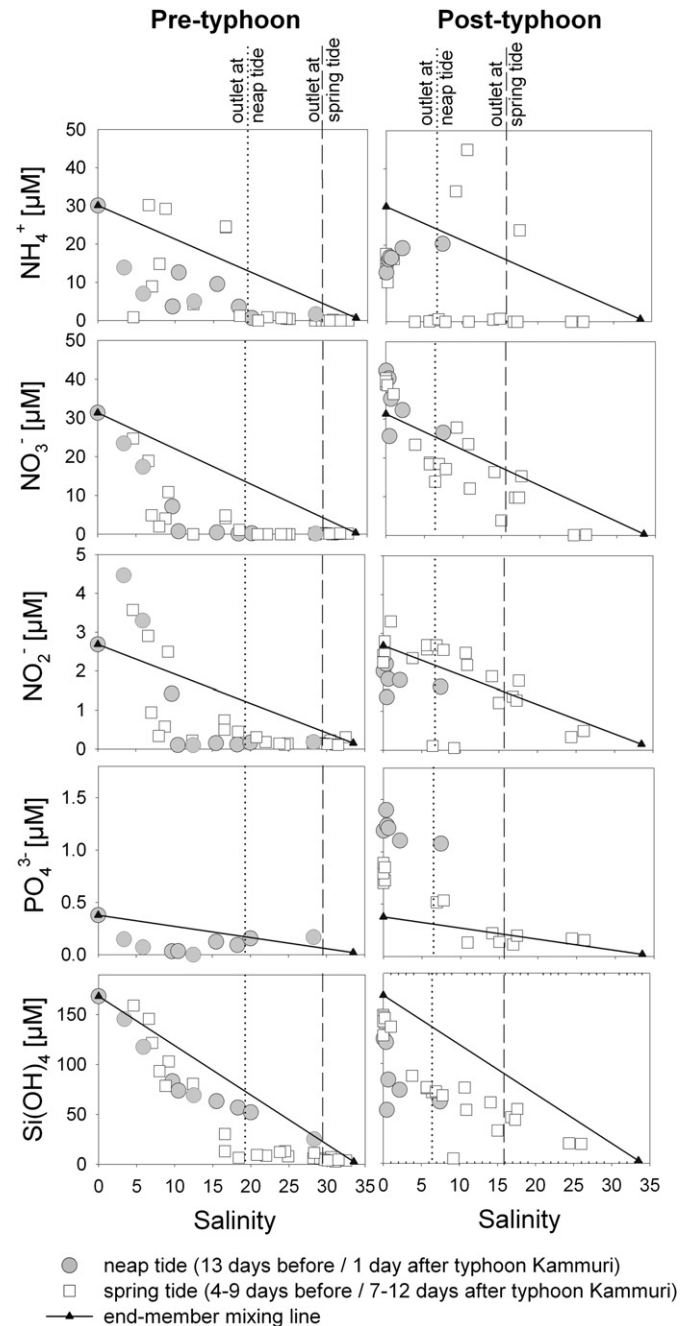

Fig. 4. Surface water concentrations of dissolved inorganic nutrients along the WWE under neap and spring tide pre-typhoon (left column) and neap and spring tide post-typhoon conditions (right column). The end-member mixing line indicates nutrient concentrations expected from conservative mixing of fresh and marine water masses with nutrient concentrations given in Table 2. Vertical dotted and dashed lines denote salinity at the outlet during neap and spring tide, respectively. Pre-typhoon phosphate concentrations during spring tide could not be determined due to sample loss.

3.2. Dissolved inorganic nutrients

Before typhoon Kammuri, all dissolved nutrients decreased along the salinity gradient during neap and spring tide resulting in low concentrations in offshore direction to the outlet (Fig. 4). Nitrate and silicate decreased sharply with increasing salinity, while there was an increase in nitrite at salinities around 5 and in ammonium at salinities between 10 and 17. In the upper estuary, nitrate dominated the DIN pool, while in the middle (and outer) estuary strong nitrate removal along the estuary accompanied with partial ammonium increases resulted in ammonium dominance in the DIN pool (Fig. 5). Ammonium concentrations above the mixing line at station A indicate temporarily high N input into the estuary causing ammonium dominance in the DIN pool during spring tide (Figs. 4 and 5).

One day after the typhoon, all nutrients decreased very little along the estuary and passed the outlet in much higher concentrations than before the typhoon (Fig. 4). Ammonium, nitrite and silicate were lower in the upper estuary compared to pre-typhoon conditions. In contrast, nitrate and phosphate concentrations in the upper estuary were greater than before the typhoon and only decreased slightly with increasing salinity. This resulted in an estuary-wide shift from ammonium to nitrate dominance in the DIN pool (Fig. 5), which was slightly attenuated toward the outer estuary because of higher ammonium concentrations with salinity (Fig. 4).

7–12 days after the typhoon, silicate and nitrite in the upper estuary were higher compared to directly after the typhoon (Fig. 4). Ammonium concentrations in the upper estuary were still similar to directly after the typhoon. In the middle and outer estuary, ammonium concentrations were low indicating effective removal in the lagoon. The few exceptions suggest local ammonium input into the lagoon. Phosphate concentrations in the upper estuary still exceeded pre-typhoon concentrations, but were lower compared to directly after the typhoon and decreased with increasing salinity.
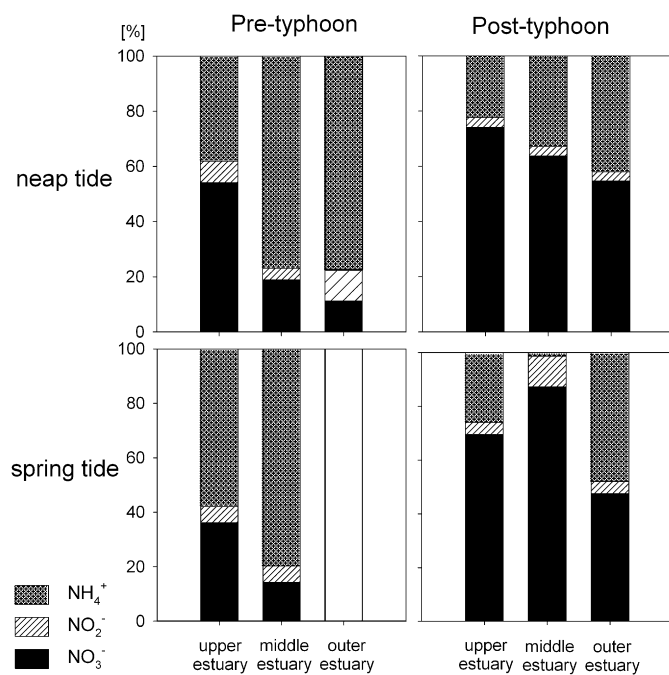
Nitrate levels in the upper estuary were still greater than before the typhoon and decreased less from station A to C compared to before the typhoon, resulting in comparatively high concentrations throughout the estuary, export of nitrate into the coast and prevailing nitrate dominance in the DIN pool in the upper and middle estuary (Fig. 5).

3.3. Suspended particulate matter concentration and composition

Under pre-typhoon conditions (neap and spring tide), TSM concentrations ranged between 8 and 43 mg l^{-1} with a TSM maximum in the middle estuary (Fig. 6a). Chl a concentrations were especially high in the middle estuary during neap tide (11–27 μg l^{-1}), while during spring tide concentrations were considerably lower (0–15 μg l^{-1}) throughout the estuary with a distinct offshore decrease (Fig. 6b). Pre-typhoon organic matter (OM) contents of the TSM at neap and spring tide were high in the upper estuary and decreased toward the coast: At neap tide, C_{org} and TN contents decreased from 20.9% to 5.4% and from 1.7% to 0.9%, respectively. Average spring tide C_{org} and TN contents were lower, decreasing from 7.6% to 3.5% and from 1.3% to 0.4% from station A to C, respectively. The C/N ratio varied from 14.0 in the upper to 5.4–9.9 in the middle and outer estuary, while average spring tide C/N ratios were more homogenous along the estuary (6.3–7.9). $\delta^{13}C_{org}$ and $\delta^{15}N$ values increased abruptly downstream of station 1 and revealed the same pattern during neap and spring tide (Fig. 6c and d).

One day after Kammuri (at neap tide), TSM concentrations had increased two- to three-fold at all stations to values between 21 and 58 mg l^{-1} (Fig. 6a), while chl a concentrations had dropped to values between 5 and 10 μg l^{-1} (Fig. 6b). C_{org} and TN contents were lower as compared to pre-typhoon contents at all stations (range: 4.8–6.2% and 0.4–0.8%, respectively). C/N ratios were higher in the middle and outer estuary (between 8 and 16), whereas in the upper estuary C/N ratios decreased from 14 to 12.4. $\delta^{13}Corg$ and $\delta^{15}N$ of TSM were higher in the upper estuary and lower in the middle and outer estuary as compared to before the typhoon, so that they were virtually uniform (approximately $-26\permil$ and $4\permil$, respectively) throughout the estuary (Fig. 6c and d).

One to two weeks after the typhoon (at spring tide), TSM concentrations had decreased to below pre-typhoon spring tide levels in the upper and middle estuary, while in the outer estuary, TSM concentrations were greater than before the typhoon (Fig. 6a). Chl a concentrations remained low in the upper estuary, while they were elevated 3- and 15-fold on average compared to pre-typhoon spring tide concentrations in the middle and outer estuary, respectively (Fig. 6b). In the middle and outer estuary, contents of C_{org} (11.0 $\pm$ 3.0 and 6.7 $\pm$ 1.6) and TN (1.9 $\pm$ 0.4 and 1.1 $\pm$ 0.3) were significantly higher compared to pre-typhoon spring tide values. Average C/N ratios were in the same range as before the typhoon in the middle (7.4 $\pm$ 0.8) and outer estuary (6.9 $\pm$ 0.6) and significantly higher compared to before Kammuri in the upper estuary (8.9 $\pm$ 0.6). $\delta^{13}C_{org}$ and $\delta^{15}N$ of TSM had returned to pre-typhoon values (Fig. 6c and d) except station A, where TSM was still significantly enriched in ^{15}N as compared to before the typhoon ($p < 0.05$).

4. Discussion

4.1. Sources and distribution of dissolved and particulate matter before the typhoon

Under 'normal' summer monsoon conditions (pre-typhoon), the distribution of dissolved and particulate matter in the WWE was dominated by the interaction of freshwater discharge and
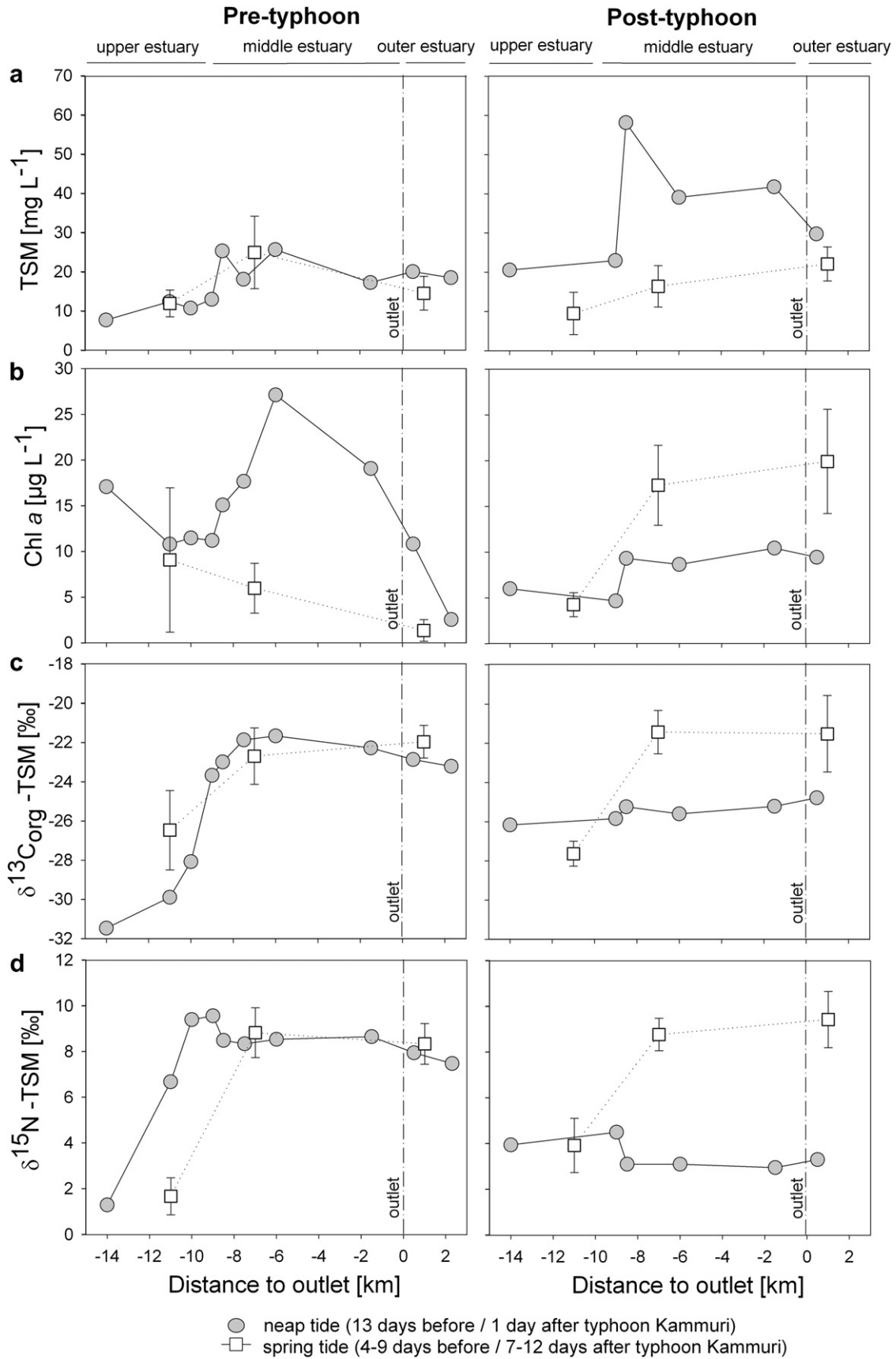

Fig. 5. Average surface water DIN composition in the upper, middle and outer estuary at neap and spring tide under pre- and post-typhoon conditions. Pre-typhoon spring tide concentrations of nitrate, nitrite and ammonium at the outer estuary were at the detection limit, so that their relative contribution to the DIN pool was meaningless.

Fig. 6. Concentration of (a) total suspended matter (TSM), (b) chlorophyll a (chl a), (c) $\delta^{13}C_{org}$-TSM and (d) $\delta^{15}N$-TSM along the WWE under neap and spring tide pre-typhoon (left column) and neap and spring tide post-typhoon conditions (right column). Spring tide samples with mean and standard deviation ($n = 8$).
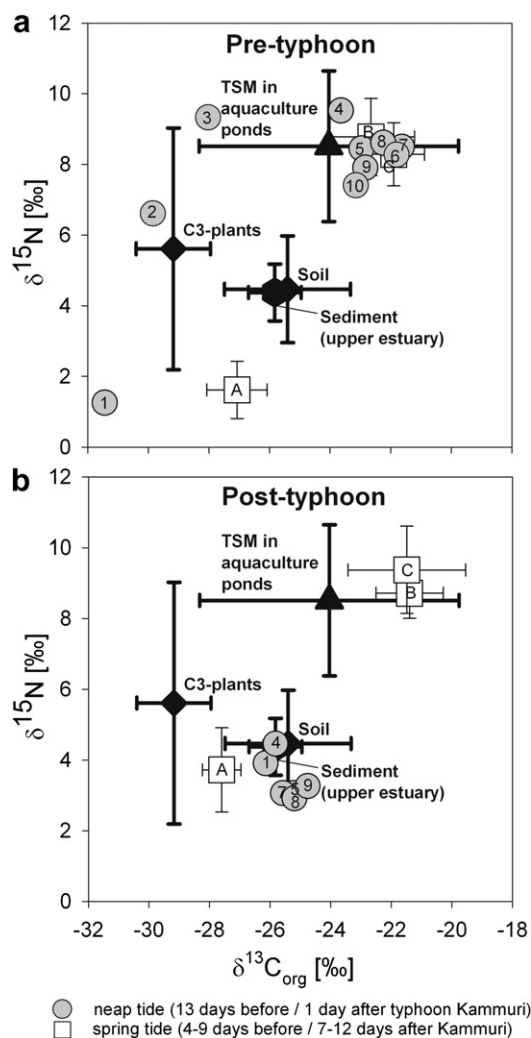
Fig. 7. (a) Pre-typhoon and (b) post-typhoon $\delta^{13}C_{org}$ vs. $\delta^{15}N$ of estuarine TSM at neap tide stations (1–10) and spring tide stations (A–C) and of selected potential end-members as listed in Table 2. Spring tide and end-member samples with mean and standard deviation. Numbers refer to station numbers in Fig. 1c.

tide-mediated variations in vertical and horizontal mixing with marine water (Fig. 3). High nutrient and particulate organic matter concentrations as well as low $\delta^{13}C_{org}$ and $\delta^{15}N$ of TSM (Fig. 7a) distinguished sources and biogeochemical composition of dissolved and particulate components in the freshwater-dominated upper estuary from the area downstream. High chl a concentrations, C_{org} and TN contents of TSM, and a very low $\delta^{13}C_{org}$ value of up to $-32‰$ indicative of freshwater phytoplankton (Martinelli et al., 1999) point toward autochthonous riverine production as primary organic matter source at station 1. A C/N ratio of 14 in combination with the occurrence of plant detritus in this sample suggest TSM at this station to mainly consist of a mixture of freshwater phytoplankton and vascular plants (e.g. limnic macrophytes, such as water hyacinths, and/or mangroves; Table 2). During neap tide, the upper estuary had a stronger fluvial/terrestrial influence (low salinity, high organic matter, high C/N ratio), while greater tidal mixing during spring tide caused a mixture of riverine TSM with TSM originating from the middle estuary (see below). C isotopes cannot tell us the origin of TSM in a definite matter but the higher mean $\delta^{13}C_{org}$ in combination with a lower C/N ratio close to the Redfield ratio at station A compared to station 2 are a strong indicator for a greater portion of marine phytoplankton (typical $\delta^{13}C_{org}$ of $-18‰$ to $-22‰$ in tropical regions; e.g. Fischer, 1991) in the TSM of the upper estuary during spring tide. The comparatively low $\delta^{15}N$ of TSM at station 1 was most likely linked to sources and processes of dissolved nitrogen in the upper catchment, as N-Input from in situ N_2-fixation by phytoplankton as source of isotopically light N can be excluded, since cyanobacterial biomass was consistently low in water samples from station 1 (D. Maier, pers. comm.). Possible processes resulting in such low $\delta^{15}N$ of TSM are strong fractionation by primary producers during N-uptake due to very high DIN concentrations (Cifuentes et al., 1988; Montoya et al., 1991; Montoya and McCarthy, 1995) and/or uptake of light nitrogen originating e.g. from Haber-process produced chemical fertilizers applied in the agriculture. Although, the N sources and processes cannot easily be separated using N isotopes alone, our data suggest that high nitrate concentrations may arise from input of agricultural fertilizers from the watershed, which are usually leached from soils in the form of nitrate (Mian et al., 2009 and references therein) and typically have a $\delta^{15}N$ of -2 to $2‰$ (e.g. Lee et al., 2008). Untreated municipal sewage from Wenchang City is another potential source of dissolved nutrients and particulate organic matter, but this should be enriched in $\delta^{15}N$

Table 2
Concentrations (mean ± SD) of potential sources (end-members) of particulate matter and inorganic nutrients in the WWE in July/August 2008. Samples were mostly taken before the passage of typhoon Kammuri.

Samples	Particulate matter				Inorganic nutrients					
	$\delta^{13}C_{org}$ [‰]	[‰] $\delta^{15}N$	C/N-ratio	n	NH_4^+ [μM]	NO_3^- [μM]	NO_2^- [μM]	PO_4^{3+} [μM]	$Si(OH)_4$[μM]	n
Typhoon rain (August 6/7, 2008)					20.4 (±12.3)	6.0 (±2.3)	0.1 (±0.1)	0.9 (±0.5)	0.7 (±0.0)	3
Freshwater (salinity = 0)	−27.2 (±3.2)	3.9 (±2.0)	8.8 (±3.5)	4	30.1	31.3	2.7	0.4	168.4	1
Marine water (salinity = 33.5)	−21.0 (±0.6)	6.1 (±0.3)	6.3 (±0.6)	4	0.7	0.3	0.0	2.6		1
Aquaculture ponds (water)	−24.0 (±4.3)	8.5 (±2.1)	6.5 (±0.2)	4	30.0 (±31.8)	0.4 (±0.7)	1.4 (±2.0)	2.2 (±1.4)	19.5 (±17.8)	8
Sediments of upper estuary (0−5 cm)	−25.8 (±0.9)	4.4 (±0.8)	9.2 (±02.5)	6	40.0 (±18.8)	2.9 (±2.9)	3.4 (±2.6)	12.1 (±5.2)	91.0 (±24.7)	8
Sediments of middle estuary (0−5 cm)	−22.8 (±2.2)	6.9 (±1.3)	15.0 (±2.7)	7	32.7 (±22.2)	0.6 (±0.5)	0.7 (±0.7)	6.4 (±2.7)	90.5 (±20.5)	10
Sediments of outer estuary (0−5 cm)	−18.0 (±0.9)	6.2 (±0.5)	9.7 (±0.4)	6						
Soils (from agriculture fields)	−25.4 (±2.1)	4.5 (±1.5)	15.4 (±4.0)	4						
C3-plants:	−27.3 (±1.4)	4.4 (±0.7)	27.0 (±4.6)	4						
mangrove leaf	−28.6 (±1.9)	3.3 (±2.2)		5						
hyacinth leaf	−28.8 (±0.8)	9.3 (±2.7)		8						
rice leaf	−29.6 (±0.9)	4.9 (±1.7)		7						
palm tree leaf	−29.4 (±1.3)	3.0 (±0.9)		6						
C4-plants:										
corn leaf	−12.3 (±0.3)	11.0 (±0.6)		3						
sugar cane leaf	−11.8 (±0.1)	5.5 (±0.3)		2						

(Costanzo et al., 2001; Lee et al., 2008), which is not reflected in the observed low $\delta^{15}N$ values of TSM. Porewater inputs from the mangrove-fringed tidal flats (Table 2) may also contribute to the nutrient inventory of the upper estuary, as it has been shown from other regions (e.g. Dittmar and Lara, 2001; Akamatsu et al., 2009). High C_{org} and TN contents in TSM and sediments and temporarily low DO concentrations suggest high remineralization rates of OM in the upper estuary. Remineralized N in porewater may potentially have low $\delta^{15}N$ values because mangroves typically have a significant amount of N_2 fixation associated with them (Holguin et al., 2001). Nitrite concentrations in the surface water above the mixing line at salinities around 5 are indicative for nitrification processes, which could also be responsible for the allocation of isotopically light nitrate. Denitrification can be neglected as an important process because DO concentrations measured were high throughout the estuarine transect. Nitrification in addition to nutrient uptake by phytoplankton and mangroves may also result in a greater removal of ammonium compared to nitrate, phosphate and silicate along the upper estuary (Fig. 4). High inputs of ammonium at station A may be related to elevated porewater export from larger inundated intertidal areas during spring tide (Dittmar and Lara, 2001) and/or local inputs of effluents from aquaculture ponds (Table 2) observed during sampling. Due to the higher contribution of nitrate to the DIN pool in the upper estuary compared to the middle and outer estuary (Fig. 5) and the very low $\delta^{15}N$ of the TSM at station 1, it is conceivable that a combination of fertilizers leached from agriculture soils and nitrified ammonium from organic matter regeneration in the sediment (some of it potentially coming from N_2-fixers in mangroves) were the main DIN sources in the upper estuary. Further studies are needed to clarify the relative relevance of each process.

In the middle and outer estuary, high C_{org} and TN values and a C/N ratio in the range of the Redfield ratio in combination with $\delta^{13}C_{org}$ values between -22 and $-24‰$ indicate TSM to be mainly of planktonic origin dominated by marine phytoplankton (Table 2; Fischer, 1991). The higher abundance of ciliates and other zooplankton at station 4 compared to all other sites (D. Maier, pers. comm.) suggests that planctonic TSM delivered by the Wenchang River (upper estuary) is mainly consumed before being transported into the lagoon and may have caused the distinct shift in $\delta^{13}C_{org}$ from the upper to the middle estuary. The strong increase of $\delta^{15}N$ of TSM from the upper to the middle estuary indicates a shift in the DIN source. The high $\delta^{15}N$ may result from uptake of ^{15}N-enriched nitrate and ammonium and/or intermixture with ^{15}N-enriched TSM, both released into the lagoon with shrimp and fish pond effluents (Fig. 7a, Table 2). Generally, elevated $\delta^{15}N$ values in particulate matter have been related to aquaculture impact in various systems (Jones et al., 2001; Costanzo et al., 2004; Lin and Fong, 2008).

In general, mixing with nutrient poor marine waters is responsible for the seaward decrease in nutrient concentrations. Additionally, non-conservative behavior of all nutrients with salinity (Fig. 4) designates strong uptake by primary producers, which is corroborated by high chl a concentrations and the predominance of planktonic organic matter in TSM. The local increase in ammonium at the lagoon stations indicates drainage of untreated effluents from abundant aquaculture ponds (Table 2) as an important source of nutrients in the middle estuary. High porewater ammonium concentrations in sediments of the middle estuary (Table 2) and a sufficiently long residence time of ~5.6 days indicate that remineralization of sedimentary organic matter may also be a relevant process for N supply to the water column in the middle estuary. Ammonium addition and simultaneous removal of nitrate in the middle estuary result in a shift in the DIN pool from nitrate dominance in the upper to ammonium dominance in the middle and outer estuary (Fig. 5).

Neap- and spring tide concentrations ≤ 1 μM ammonium, nitrate, nitrite and phosphate in the outer estuary indicate that export of dissolved inorganic nitrogen and phosphate to the coast does not allow for accumulation in coastal waters and appears therefore negligible under 'normal' summer monsoon conditions. Silicate, which in contrast to all other nutrients determined is not related to anthropogenic emission, was the only dissolved nutrient exported into coastal waters. This implies that the WWE acts as a sink for dissolved N and P derived from land, and released from aquaculture ponds or from internal nutrient regeneration. This filter function is facilitated by the morphology of the middle estuary (medium-sized lagoon with a narrow inlet channel) that hampers the immediate outflow and mixing with coastal marine waters and thus fosters the uptake of nutrients by brackish-water phytoplankton, its consumption by organisms of higher trophic levels, as well as deposition in sediments within the lagoon. This filtering capacity of the estuary is most likely an important prerequisite allowing the development of coral reefs and seagrass meadows in close vicinity to the lagoon despite continuous riverine nutrient and sediment input, and may buffer the adverse effects of additional inputs from aquaculture sources.

4.2. Sources and distribution of dissolved and particulate matter during and after the typhoon

Typhoon-associated rains enhanced river discharge and turned the estuary into a river-dominated system, as documented by the reduction of salinity during and after the typhoon (Fig. 3; Table 1).

One day after the typhoon, seawater intrusion into the lagoon was essentially restricted to the bottom layer and the estuarine salinity gradient was shifted toward the coastal sea (Fig. 3). This indicates that rain water inputs caused an almost complete flushing of the lagoon; intrusion of marine waters triggered by typhoon-induced wind and wave forcing through the inlet channel was not evident. The relatively uniform distribution of physico-chemical properties, nutrients and TSM concentration and composition along the transect sampled indicates that due to extreme runoff, dissolved and particulate matter from the upper catchment dominated in the entire estuary and was eventually exported into coastal waters. A high similarity in $\delta^{13}C_{org}$ and $\delta^{15}N$ values of TSM and C3 plants, upstream sediments and soils from the watershed designates terrestrial matter as a major organic matter source of TSM after the typhoon (Fig. 7b). C/N ratios of TSM between 8 and 16 specify soils as the most likely source of suspended matter (Table 2). This implies that the torrential rainfall increased erosion of the predominantly agricultural soils in the upper catchment leading to a high input of allochthonous particles into the lagoon and coastal zone. Post-hurricane $\delta^{15}N$ values around 4‰ were also observed in the Pamlico Sound System and also ascribed to such processes (Paerl et al., 2006a). Typhoon-derived soil erosion also had a dominant impact on $\delta^{15}N$-TSM in the eutrophic Danshuei Estuary in northern Taiwan (Chen et al., 2001; Liu et al., 2007), causing $\delta^{15}N$ values to rise to $>2‰$, where under normal conditions high fractionation during planktonic uptake led to a very low $\delta^{15}N$ signal ($<0‰$). Wind-driven sediment resuspension along the shallow margins of the lagoon may also play a role, however dissimilarity in the $\delta^{13}C_{org}$ and $\delta^{15}N$ of TSM and lagoon sediments (Table 2) proofs that this process is likely of minor importance. Reduced chl a concentrations and lower C_{org} and TN contents 1 day after the typhoon reflect that the rich phytoplankton population of the lagoon was pushed seaward with the first flush after the precipitation event. Homogenous and elevated nutrient levels along the sampled transect suggest that nutrient uptake by phytoplankton was restricted. Reduced concentrations of silicate after the typhoon indicate dilution of

brackish waters with rain water containing low levels of silicate (Table 2). Concentrations of ammonium along the transect were in the range of ammonium in rain water, but nitrate concentrations in the water column were 3–11 times higher than in rain water. This indicates that in addition to direct atmospheric inputs of reactive nitrogen by rain (Table 2), which can be a significant 'new' N source in estuaries after heavy rains (Paerl, 1985; Paerl and Fogel, 1994), especially along the Chinese coast (e.g. Duce et al., 2008), nitrate was leached from agricultural fields in high quantities by a massive freshwater input, leading to a strong enhancement in nitrate concentrations after the typhoon. Peierls et al. (2003) also related an increase of nitrate in Pamlico Sound in the wake of a hurricane to freshwater input. The increase in phosphate is probably also linked to leaching from agricultural soils, though, phosphate concentrations may have declined through adsorption onto the typhoon-derived larger amount of particulates in the water column. In contrast, typhoon-related resuspension of estuarine sediments and associated release of nitrate and ammonium from sediment pore-water into the water column was probably negligible compared to the afore-mentioned external nutrient inputs: a theoretical release of porewater from a 1 m^2 wide and 5 cm deep sediment layer having an assumed porosity of 0.6 and porewater concentrations as listed in Table 2 into a overlying water column of 3.5 m depth would only have augmented water nutrient concentrations by <1% relative to pre-typhoon concentrations. Therefore, nitrate from agriculture soils and rain inputs are considered the major source of dissolved nitrogen replacing aquaculture-derived ammonium before the typhoon and causing a shift in the DIN pool toward nitrate dominance in the middle and outer estuary after the typhoon (Fig. 5). High nutrient concentrations measured at station 9 directly after the typhoon indicate that nutrients were not completely consumed inside the estuarine lagoon, as usual. Nutrient uptake inside the lagoon by phytoplankton was restricted due to the short residence time during typhoon-associated flushing and light limitation resulting from high loads of allochthonous TSM in the water column, as reflected by low Secchi depths (Table 1). Hence, the typhoon-induced flushing of the estuarine lagoon led to an export of nutrients into the outer estuary and fertilization of the coastal zone, so that under typhoon conditions the WWE acted as a nutrient source toward the coastal sea.

Two weeks after Kammuri's passage, the biogeochemical conditions in the estuarine system had started to return to pre-typhoon conditions. However, a comparison of physico-chemical properties and dissolved nutrients 1–2 weeks after the typhoon with pre-typhoon values (both at spring tide) illustrates the persistent impact of the flushing. Relatively low surface and bottom water salinities despite spring tide conditions designate that typhoon-induced runoff was still draining from the watershed causing diminished impact of tidal forcing and a seaward shift of the estuarine gradient (Figs. 3 and 4). Reduction of silicate, ammonium and phosphate with salinity to levels below the end-member mixing line indicate nutrient removal by phytoplankton and other primary producers along the estuarine transect, as observed before the typhoon. However, elevated nitrate and phosphate concentrations compared to pre-typhoon spring tide conditions indicate that the supply of nutrients from the upper catchment into the estuary continued. High nitrite levels suggest nitrification, which may have resulted from recycling of organic matter transported into the estuary with precipitation runoff. Also after the typhoon, denitrification appears to be unlikely because of relatively high DO concentrations (Table 1). Nitrate inputs from land accompanied by nitrification processes accounted for the persisting dominance of nitrate in the DIN pool one to two weeks after the typhoon (Fig. 5). Higher silicate levels in the upper estuary compared to directly after the typhoon indicate increased silicate

inputs from land. In contrast, TSM concentrations were even lower than before the typhoon in the upper and middle estuary and the isotope composition distinguishes particulate organic matter from the upper estuary from that of the middle and lower estuary, as it was under pre-typhoon conditions (Fig. 7). This suggests a first flush effect: Only the initial freshwater pulse delivered considerable amounts of eroded soils and sediments into the estuary. Within a few days after the typhoon's passage, these allochthonous particles were to a large extent exported offshore favored by the strong ebb dominance in the lagoon during spring tide and/or removed from the water column of the lagoon by rapidly settling particles (e.g. Victor et al., 2006). Resultant relief from light limitation, as indicated by the increased Secchi depth, together with the ample nutrient availability, stimulated phytoplankton growth in the middle and in particular in the outer estuary. This was evident from increased concentrations of chl *a* and DO, a $\delta^{13}C_{org}$ signal typical for estuarine/marine phytoplankton and low ammonium and phosphate levels at these sites.

4.3. Relevance of typhoon precipitation for the estuarine system and nearshore coastal zone

Our results show that the nutrient input to coastal waters is very low at 'normal' low discharge, despite significant land use changes along the estuary and in the watershed (Fig. 8a). Under these conditions, the estuary acts as a sink for dissolved nitrogen and phosphorus due to high nutrient uptake by primary producers inside the lagoon. Strong alterations in the amount and composition of dissolved nutrients and total suspended matter in the WWE after typhoon Kammuri showed that heavy precipitation had significant effects on the estuarine biogeochemistry persisting over several weeks. It caused increased soil erosion in the catchment and flooding of the estuarine lagoon with nutrient- and sediment-laden freshwater (Fig. 8b). Thus, the estuarine filter function was interrupted for several days until most of the precipitation runoff had passed through the estuary. Nutrients derived from agriculture, aquaculture and urban effluents and organic matter regeneration, which are normally retained inside the estuarine lagoon, are then exported into coastal areas together with additional atmospheric nutrient inputs through rain (Fig. 8b and c). During and after major precipitation events, the estuary represents a temporal source of nutrients and organic matter toward the coastal ocean lasting for at least two weeks. The fertilization of the coastal ocean stimulated phytoplankton growth within a few days after the initial freshwater pulse. Phytoplankton blooms induced by increased N loadings have been observed in a range of estuaries and coastal seas worldwide several days after major storms (e.g. Valiela et al., 1998; Paerl et al., 2001, 2006a; Peierls et al., 2003; Burkholder et al., 2004; Wetz and Paerl, 2008; Zhang et al., 2009; Zhao et al., 2009). Consequences of excessive phytoplankton growth are well known and include proliferation of toxic algal species and hypoxic conditions (e.g. Paerl, 1988; Anderson et al., 2002; Livingston, 2007).

This study showed that even comparatively moderate and distant typhoons, as observed here, can induce a rapid export of freshwater, excess nutrients and TSM into nearshore regions, resulting in hyposalinity, reduced water transparency, siltation, as well as temporary eutrophication. Major storms can also cause other extreme conditions besides strong precipitation, such as seiching and other wind-driven effects. These were not observed during this study because of the relatively distant passage of Kammuri. During greater typhoon exposure (e.g. a direct typhoon landing), the estuary and coastal zone may be impacted by large storm surges resulting in sediment and nutrient resuspension or hypersalinity, as e.g observed in Breton Sound (Louisiana) after Hurricane Katrina (Piazza and Peyre, 2009). Though, it is likely that
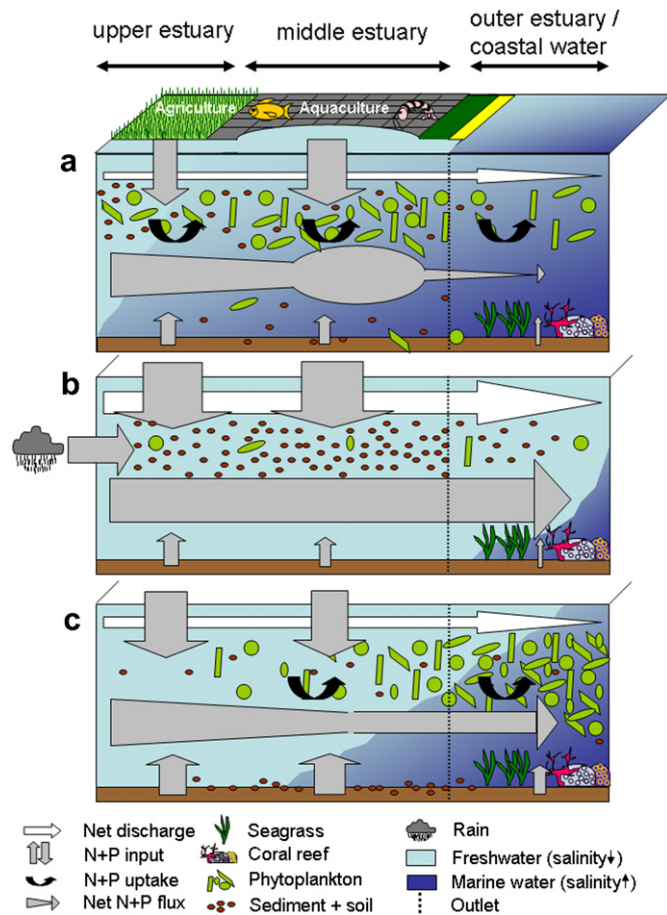
Fig. 8. Simplified sketch summarizing the major biogeochemical processes in the WWE (a) before, (b) directly after and (c) 1–2 weeks after the typhoon. (a) Before the typhoon, the salinity gradient ranges over the whole estuary, the net discharge is relatively low and dissolved N and P released into the estuary from agriculture, aquaculture and benthic recycling are taken up by phytoplankton leading to a low export of N and P to the outer estuary. (b) Directly after the typhoon, heavy precipitation causes a dominance of freshwater along the estuarine system, an increased net discharge and high amounts of allochthonous particles (sediment and soil) derived from erosion in the upper catchment. Added nutrients from rain and leaching of agricultural fields are exported to the outer estuary. They cannot be taken up by phytoplankton because it was flushed out. (c) 1–2 weeks after the typhoon, freshwater prominence and net discharge were lower enabling settlement of the allochthonous particles and subsequently the recurrence of phytoplankton. They consume introduced nutrients along the estuary, which results in a lower but still evident export of N to coastal waters.

in the WWE the relatively narrow inlet channel and adjacent fringing reefs serving as wave breakers to some extent limit the marine influence in the lagoon during typhoons.

Long-term precipitation data (Fig. 2a) reveal that pulsed rainfall events of comparable and even larger intensity frequently occur in the region. They are not necessarily related to typhoons but may also be linked to monsoonal thunderstorms. These pulsed natural disturbances are an inherent part of the overall system dynamics and most probably an important control of nutrient and material fluxes in the WWE. Because of the random occurrence of tropical storms and logistic constraints to investigate their effects, the latter are rarely accounted for in estuarine carbon and nutrient budgets. Due to a lack of some physical factors (e.g. local precipitation, river flow, etc.) we were not able to calculate nutrient and TSM fluxes. However, our biogeochemical data clearly reflected estuarine-wide changes in the water column in the wake of such an event and emphasized the quantitative significance of tropical storms for carbon and nutrient budgets.

As our data only show partial recovery of the estuarine system within 7–12 days after the typhoon, we conclude that full recovery from a typhoon of the Kammuri type to 'normal' water column conditions will take longer than 2 weeks. The similarity between salinity, nutrient and chl a concentrations 1–2 weeks after the typhoon (during spring tide) and neap tide concentrations before the typhoon emphasizes that it is important to consider both tidal phases (spring and neap tide) to distinguish typhoon effects from tidal variations and to clearly evaluate the recovery time of a system. This, however, is seldomly accounted for in other studies. The duration of recovery of an estuarine system is generally related to precipitation rates and frequency of rain events, as well as morphologic (e.g. size of watershed and estuary), hydrologic (e.g. flushing and residence times) and other regional factors. Due to the relatively short water residence time of ~5.6 days and the small catchment size, it is conceivable that the recovery time of the WWE is at the lower end of the range reported in other studies varying between days (e.g. Valiela et al., 1998), months (e.g. Zhang et al., 2009) and years (e.g. Paerl et al., 2001; Burkholder et al., 2004).

Hainan's seagrasses and coral reefs are under stress from overfishing, habitat destruction and pollution (Hutchings and Wu, 1987; Fiege et al., 1994; Huang et al., 2006). The episodic flushing of freshwater, excess nutrients and organic matter into coastal waters we observed can additionally impair the performance of adjacent seagrass meadows and coral reefs, which are adapted to oligotrophic conditions. Besides direct physiological stress from siltation, low light availability and hyposalinity, the nutrient pulses can stimulate excessive growth of benthic algae, which may ultimately result in a phase shift in coral reefs and seagrass meadows toward algal dominance (e.g. Valiela et al., 1997; McCook, 1999). It is likely that during recent decades the detrimental effects of estuarine flushing have been significantly reinforced by the anthropogenically enhanced nutrient and organic matter input from expanding agriculture and aquaculture and the loss of wetland areas, which under natural conditions act as a buffer retaining nutrients and sediments (Valiela and Cole, 2002; Walsh and Nittrouer, 2004; Victor et al., 2004; Wolanski, 2007). China lost about 50% of its coastal wetlands between 1950 and 2000 (An et al., 2007). Besides that, the loss of wetlands and flood plains fostered by e.g. the construction of aquaculture ponds accelerates runoff velocity and thereby aggravates typhoon effects. Projected increase in typhoon intensity, duration and possibly frequency (e.g. Knutson et al., 2010) in combination with enhanced nutrient and sediment inputs into the estuary related to human activities in the catchment will expose the estuarine and coastal habitats more often and for longer time periods to eutrophication and hyposalinity stress, thereby extending their recovery time and eventually weakening their resilience.

References

Akamatsu, Y., Ikeda, S., Toda, Y., 2009. Transport of nutrients and organic matter in a mangrove swamp. Estuarine, Coastal and Shelf Science 82, 233–242.

Alongi, D.M., 2002. Present state and future of the world's mangrove forests. Environmental Conservation 29 (3), 331–349.

An, S., Li, H., Guan, B., Zhou, C., Wang, Z., Deng, Z., Zhi, Y., Liu, Y., Xu, C., Fang, S., Jiang, J., Li, H., 2007. China's natural wetlands: past problems, current status, and future challenges. Ambio 36 (4), 335–342.

Anderson, D.M., Glibert, P.M., Burkholder, J.M., 2002. Harmful algal blooms and eutrophication: nutrient sources, composition, and consequences. Estuaries and Coasts 25 (4), 704–726.

Burkholder, J., Eggleston, D., Glasgow, H., Brownie, C., Reed, R., Janowitz, G., Posey, M., Melia, G., Kinder, C., Corbett, R., Toms, D., Alphin, T., Deamer, N., Springer, J., 2004. Comparative impacts of two major hurricane seasons on the Neuse River and western Pamlico Sound ecosystems. Proceedings of the National Academy of Sciences 101, 9291–9296.

Chen, K.L., Kao, S.J., Liu, K.K., 2001. Fluxes and isotopic compositions of particulate organic carbon and nitrogen from the Tamshui River during typhoon flood. Acta Oceanographica Taiwanica 39, 219–232 (in Chinese).

Cifuentes, L.A., Sharp, J.H., Fogel, M.L., 1988. Stable carbon and nitrogen isotope biogeochemistry in the Delaware estuary. Limnology and Oceanography 33, 1102–1115.

Climate Center, Precipitation data for Haikou and Qionghai, 2000–2008, Utah State University, online, dataset, 2011; http://climate.usurf.usu.edu/products/data.php?tab=gsod.

Costanzo, S.D., O'Donohue, M.J., Dennison, W.C., Loneragan, N.R., Thomas, M., 2001. A new approach for detecting and mapping sewage impacts. Marine Pollution Bulletin 42, 149–156.

Costanzo, S.D., O'Donohue, M.J., Dennison, W.C., 2004. Assessing the influence and distribution of shrimp pond effluent in a tidal mangrove creek in north-east Australia. Marine Pollution Bulletin 48, 514–525.

Diaz, R.J., Rosenberg, R., 2008. Spreading dead zones and consequences for marine ecosystems. Science 321, 926–929.

Dittmar, T., Lara, R.J., 2001. Driving forces behind nutrient and organic matter dynamics in a mangrove tidal creek in North Brazil. Estuarine, Coastal and Shelf Science 52, 249–259.

Duce, R.A., LaRoche, J., Altieri, K., Arrigo, K.R., Baker, A.R., Capone, D.G., Cornell, S., Dentener, F., Galloway, J., Ganeshram, R.S., Geider, R.J., Jickells, T., Kuypers, M.M., Langlois, R., Liss, P.S., Liu, S.M., Middelburg, J.J., Moore, C.M., Nickovic, S., Oschlies, A., Pedersen, T., Prospero, J., Schlitzer, R., Seitzinger, S., Sorensen, L.L., Uematsu, M., Ulloa, O., Voss, M., Ward, B., Zamora, L., 2008. Impacts of atmospheric anthropogenic nitrogen on the open ocean. Science 320, 893–897.

Emanuel, K., 2005. Increasing destructiveness of tropical cyclones over the past 30 years. Nature 436, 686–688.

Fiege, D., Neumann, V., Li, J., 1994. Observations on coral reefs of Hainan island, South China sea. Marine Pollution Bulletin 29, 84–89.

Fink, A.H., Speth, P., 1998. Tropical cyclones. Naturwissenschaften 85, 483–493.

Fischer, G., 1991. Stable carbon isotope ratios of plankton carbon and sinking organic matter from the Atlantic sector of the Southern Ocean. Marine Chemistry 35, 581–596.

Goldenberg, S.B., Landsea, C.W., Mestas-Nunez, A.M., Gray, V.M., 2001. The recent increase in Atlantic hurricane activity: causes and implications. Science 293, 474–479.

Goldsmith, S.T., Carey, A.E., Berry Lyons, W., Kao, S.-J., Lee, T.-Y., Chen, J., 2008. Extreme storm events, landscape denudation, and carbon sequestration: typhoon Mindulle, Choshui River, Taiwan. Geology 36, 483–486.

Grasshoff, K., Kremling, K., Ehrhardt, M. (Eds.), 1999. Methods of Seawater Analysis, third ed. Wiley-VCH, Weinheim, p. 600.

Hilton, R.G., Galy, A., Hovius, N., Chen, M.-C., Horng, M.-J., Chen, H., 2008. Tropical-cyclone-driven erosion of the terrestrial biosphere from mountains. Nature Geoscience 1, 759–762.

Holguin, G., Vazquez, P., Bashan, Y., 2001. The role of sediment microorganisms in the productivity, conservation, and rehabilitation of mangrove ecosystems: an overview. Biology and Fertility of Soils 33, 265–278.

Huang, L., 2003. Conflicts between ecology and economy and possible solutions: a case study from Hainan Province, South-China. Dissertation, Freiburg (Breisgau)-University, 310 pp. (in German). http://www.freidok.uni-freiburg.de/volltexte/1349/pdf/OekoHL08.pdf.

Huang, X., Huang, L., Li, Y., Xu, Z., Fong, C.W., Huang, D., Han, Q., Huang, H., Tan, Y., Liu, S., 2006. Main seagrass beds and threats to their habitats in the coastal sea of South China. Chinese Science Bulletin 51, 136–142.

Hutchings, P.A., Wu, B.L., 1987. Coral reefs of Hainan island, South China sea. Marine Pollution Bulletin 18, 25–26.

Jones, A.B., O'Donohue, M.J., Udy, J., Dennison, W.C., 2001. Assessing ecological impacts of shrimp and sewage effluent: biological indicators with standard water quality analysis. Estuarine, Coastal and Shelf Science 52, 91–109.

Justic, D., Rabalais, N.N., Turner, R.E., 2002. Modeling the impacts of decadal changes in riverine nutrient fluxes on coastal eutrophication near the Mississippi river delta. Ecological Modelling 152, 33–46.

Kao, S.-J., Liu, K.-K., 1996. Particulate organic carbon export from a subtropical mountainous river (Langyang Hsi) in Taiwan. Limnology and Oceanography 4, 1749–1757.

Kitamoto A. General information on Typhoon Kammuri 200809, August 2008. National Institute of Informatics (NII), Japan, online, dataset, May 2011; http://agora.ex.nii.ac.jp/digital-typhoon/summary/wnp/s/200809.html.en.

Knutson, T.R., McBride, J.L., Chan, J., Emanuel, K., Holland, G., Landsea, C., Held, I., Kossin, J.P., Srivastava, A.K., Sugi, M., 2010. Tropical cyclones and climate change. Nature Geoscience 3, 157–163.

Krumme, U., Herbeck, L.S., Wang, T.C., under review. Tide- and rainfall-induced variations of physical and chemical parameters in a mangrove-depleted estuary of East Hainan (South China Sea).

Lee, K.-S., Bong, Y.-S., Lee, D., Kim, Y., Kim, K., 2008. Tracing the sources of nitrate in the Han River watershed in Korea, using δ^{15}N-NO3- and δ^{18}O-NO3- values. Science of the Total Environment 395, 117–124.

Li, M.S., Lee, S.Y., 1997. Mangroves of China: a brief review. Forest Ecology and Management 96, 241–259.

Lin, D.T., Fong, P., 2008. Macroalgal indicators (growth, tissue N, δ^{15}N) detect nutrient enrichment from shrimp farm effluents entering Opunohu Bay, Moorea, French Polynesia. Marine Pollution Bulletin 56, 245–249.

Lin, I., Liu, W.T., Wu, C.C., Wong, G.T.F., Hu, C., Chen, Z., Liang, W.D., Yang, Y., Liu, K.K., 2003. New evidence for enhanced ocean primary production triggered by tropical cyclone. Geophysical Research Letters 30, 1718.

Liu, K.-K., Kao, S.-J., Wen, L.-S., Chen, K.-L., 2007. Carbon and nitrogen isotopic composition of particulate organic matter and biogeochemical processes in the eutrophic Danshuei Estuary in northern Taiwan. Science of the Total Environment 382, 103–120.

Livingston, R.J., 2007. Phytoplankton bloom effects on a Gulf estuary: water quality changes and biological response. Ecological Applications 17, 110–128.

Lorenzen, C.J., 1967. Determination of chlorophyll and pheo-pigments: spectrophotometric equations. Limnology and Oceanography 12, 343–346.

Mallin, M.A., Corbett, C.A., 2006. How hurricane attributes determine the extent of environmental effects: multiple hurricanes and different coastal systems. Estuaries and Coasts 29, 1046–1061.

Mallin, M.A., Posey, M.H., Shank, G.C., McIver, M.R., Ensign, S.H., Alphin, T.D., 1999. Hurricane effects on water quality and benthos in the Cape Fear Watershed: natural and anthropogenic impacts. Ecological Applications 9, 350–362.

Martinelli, L.A., Ballester, M.V., Krusche, A.V., Victoria, R.L., Camargo, P.B., Bernardes, M., Ometto, J.P.H.B., 1999. Land cover change and δ^{13}C composition of riverine particulate organic matter in the Piracicaba River Basin (southeast region of Brazil). Limnology and Oceanography 44, 1826–1833.

McCook, L.J., 1999. Macroalgae, nutrients and phase shifts on coral reefs: scientific issues and management consequences for the Great Barrier Reef. Coral Reefs 18, 357–367.

Mian, I.A., Riaz, M., Cresser, M.S., 2009. The importance of ammonium mobility in nitrogen-impacted unfertilized grasslands: a critical reassessment. Environmental Pollution 157 (4), 1287–1293.

Milliman, J.D., Kao, S.-J., 2005. Hyperpycnal discharge of fluvial sediment to the ocean: impact of super-typhoon Herb (1996) on Taiwanese Rivers. Journal of Geology 113, 503–516.

Milliman, J.D., Lin, S.W., Kao, S.J., Liu, J.P., Liu, C.S., Chiu, J.K., Lin, Y.C., 2007. Short-term changes in seafloor character due to flood-derived hyperpycnal discharge: typhoon Mindulle, Taiwan, July 2004. Geology 35, 779–782.

Montoya, J.P., McCarthy, J.J., 1995. Isotopic fractionation during nitrate uptake by phytoplankton grown in continuous culture. Journal of Plankton Research 17, 439–464.

Montoya, J.P., Horrigan, S.G., McCarthy, J.J., 1991. Rapid, storm-induced changes in the natural abundance of ^{15}N in a planktonic ecosystem, Chesapeake Bay, USA. Geochimica et Cosmochimica Acta 55, 3627–3638.

Paerl, H.W., 1985. Enhancement of marine primary production by nitrogen-enriched acid rain. Nature 315, 747–749.

Paerl, H.W., 1988. Nuisance phytoplankton blooms in coastal, estuarine, and inland waters. Limnology and Oceanography 33, 823–847.

Paerl, H.W., Fogel, M.L., 1994. Isotopic characterization of atmospheric nitrogen inputs as sources of enhanced primary production in coastal Atlantic Ocean waters. Marine Biology 119, 635–645.

Paerl, H.W., Bales, J.D., Ausley, L.W., Buzzelli, C.P., Crowder, L.B., Eby, L.A., Fear, J.M., Go, M., Peierls, B.L., Richardson, T.L., Ramus, J.S., 2001. Ecosystem impact of three sequential hurricanes (Dennis, Floyd, and Irene) on the United States' largest lagoonal estuary, Pamlico Sound, N.C. Proceeding of the National Academy of Sciences 98, 5655–5660.

Paerl, H.W., Valdes, L.M., Joyner, A.R., Peierls, B.L., Piehler, M.F., Riggs, S.R., Christian, R.R., Eby, L.A., Crowder, L.B., Ramus, J.S., Clesceri, E.J., Buzzelli, C.P., Luettich Jr., R.A., 2006a. Ecological response to hurricane events in the Pamlico Sound System, North Carolina and implications for assessment and management in a regime of increased frequency. Estuaries and Coasts 29, 1033–1045.

Paerl, H.W., Valdes, L.M., Peierls, B.L., Adolf, J.E., Harding, L.W., 2006b. Anthropogenic and climatic influences on the eutrophication of large estuarine ecosystems. Limnology and Oceanography 51, 448–462.

Peierls, B.L., Christian, R.R., Paerl, H.W., 2003. Water quality and phytoplankton as indicators of hurricane impacts on a large estuarine ecosystem. Estuaries 26 (5), 1329–1343.

Piazza, B.P., La Peyre, M.K., 2009. The effect of Hurricane Katrina on nekton communities in the tidal freshwater marshes of Breton Sound, Louisiana, USA. Estuarine, Coastal and Shelf Science 83, 97–104.

Rabalais, N.N., Gilbert, D., 2009. Distribution and consequences of hypoxia. In: Urban, E., Sundby, B., Malanotte-Rizzoli, P., Melillo, J.M. (Eds.), Watersheds, Bays and Bounded Seas: The Science and Management of Semi-enclosed Marine Systems. Island Press, Washington DC, pp. 2009–2226.

Seitzinger, S.P., Kroetze, C., Bouwman, A.F., Caraco, N., Dentener, F., Styles, R.V., 2002. Global patterns of dissolved inorganic and particulate nitrogen inputs to coastal systems: recent conditions and future projections. Estuaries 25, 640–655.

Shiah, F.-K., Chung, S.-W., Kao, S.-J., Gong, G.-C., Liu, K.-K., 2000. Biological and hydrographical responses to tropical cyclones (typhoons) in the continental shelf of the Taiwan Strait. Continental Shelf Research 20, 2029–2044.

Sun, L., Yang, Y.J., Xian, T., Lu, Z.M., Fu, Y.-F., 2010. Strong enhancement of chlorophyll *a* concentration by a weak typhoon. Marine Ecology Progress Series 404, 39–50.

Thampanya, U., Vermaat, J.E., Sinsakul, S., Panapitukkul, N., 2006. Coastal erosion and mangrove progradation of Southern Thailand. Estuarine, Coastal and Shelf Science 68, 75–85.

Turner, R.E., Rabalais, N.N., 1994. Coastal eutrophication near the Mississippi river delta. Nature 368, 619–621.

Uncles, R.J., Stephens, J.A., Smith, R.E., 2002. The dependence of estuarine turbidity on tidal intrusion length, tidal range and residence time. Continental Shelf Research, 1835–1856.

Valiela, I., Cole, M.L., 2002. Comparative evidence that salt marshes and mangroves may protect seagrass meadows from land-derived nitrogen loads. Ecosystems 5, 92–102.

Valiela, I., McClelland, J., Hauxwell, J., Behr, P.J., Hersh, D., Foreman, K., 1997. Macroalgal blooms in shallow estuaries: Controls and ecophysiological and ecosystem consequences. Limnology and Oceanography 42, 1105–1118.

Valiela, I., Peckol, P., D'Avanzo, C., Kremer, J., Hersh, D., Foreman, K., Lajtha, K., Seely, B., Geyer, W.R., Isaji, T., Crawford, R., 1998. Ecological effects of major storms on coastal watersheds and coastal waters: hurricane Bob on Cape Cod. Journal of Coastal Research 14, 218–238.

Verardo, D.J., Froelich, P.N., McIntyre, A., 1990. Determination of organic carbon and nitrogen in marine sediments using the Carlo Erba NA-1500 Analyzer. Deep-Sea Research 37, 157–165.

Victor, S., Golbuu, Y., Wolanski, E., Richmond, R.H., 2004. Fine sediment trapping in two mangrove-fringed estuaries exposed to contrasting land-use intensity, Palau, Micronesia. Wetlands Ecology and Management 12, 277–283.

Victor, S., Neth, L., Golbuu, Y., Wolanski, E., Richmond, R.H., 2006. Sedimentation in mangroves and coral reefs in a wet tropical island, Pohnpei, Micronesia. Estuarine, Coastal and Shelf Science 66, 409–416.

Vitousek, P.M., Aber, J.D., Howarth, R.W., Likens, G.E., Matson, P.A., Schindler, D.W., Schlesinger, W.H., Tilman, D.G., 1997. Human alteration of the global nitrogen cycle: sources and consequences. Ecological Applications 7, 737–750.

Walsh, J.P., Nittrouer, C.A., 2004. Mangrove-bank sedimentation in a mesotidal environment with large sediment supply, Gulf of Papua. Marine Geology 208, 225–248.

Wang, Y., 2002. Environmental characteristics of Hainan Island coast. Marine Geology Letters 18 (3), 1–9 (in Chinese).

Wang, Y.-M., Ren, F.-M., Li, W.-J., Wang, X.-L., 2008. Climatic characteristics of typhoon precipitation over China. Journal of Tropical Meteorology 14, 125–128.

Wang, B., Yang, Y., Ding, Q.-H., Murakami, H., Huang, F., 2010. Climate control of the global tropical storm days (1968-2008). Geophysical Research Letters 37 n.p.

Wattayakorn, G., Wolanski, E., Kjerfve, B., 1990. Mixing, trapping and outwelling in the Klong Ngao mangrove swamp, Thailand. Estuarine, Coastal and Shelf Science 31, 667–688.

Webster, P.J., Holland, G.J., Curry, J.A., Chang, H.R., 2005. Changes in tropical cyclone number, duration, and intensity in a warming environment. Science 309, 1844–1846.

Wetz, M.S., Paerl, H.W., 2008. Estuarine phytoplankton responses to hurricanes and tropical storms with different characteristics (trajectory, rainfall, winds). Estuaries and Coasts 31, 419–429.

Wolanski, E., 2007. Estuarine Ecohydrology. Elsevier, Amsterdam, 157 pp.

Wolanski, E., Richmond, R.H., Davis, G., Bonito, V., 2003. Water and fine sediment dynamics in transient river plumes in a small, reef-fringed bay, Guam. Estuarine, Coastal and Shelf Science 56, 1029–1040.

Wu, L., Wang, B., Geng, S., 2005. Growing typhoon influence on East Asia. Geophysical Research Letters 32 n.p.

Ye, L., 1988. A typical estuary consisting of a tidal inlet and lagoon system and its engineering significance. Estuaries 11, 250–254.

Zeng, Z.X., Zeng, X.Z., 1989. Nature Geography of Hainan Island. Science Press, Beijing (in Chinese).

Zhang, J.-Z., Kelble, C.R., Fischer, C.J., Moore, L., 2009. Hurricane Katrina induced nutrient runoff from an agricultural area to coastal waters in Biscayne Bay, Florida. Estuarine, Coastal and Shelf Science 84, 209–218.

Zhao, H., Tang, D.L., Wang, D., 2009. Phytoplankton blooms near the Pearl River estuary induced by typhoon Nuri. Journal of Geophysical Research 114, C12027.

Zheng, G.M., Tang, D.L., 2007. Offshore and nearshore chlorophyll increases induced by typhoon winds and subsequent terrestrial rainwater runoff. Marine Ecology Progress Series 333, 61–74.